Applied Clay Science 64 (2012) 44–52

Contents lists available at SciVerse ScienceDirect

Applied Clay Science

journal homepage: www.elsevier.com/locate/clay

Formation of soils with fragipan and plinthite in old beach deposits in the South of the Caspian Sea, Gilan province, Iran

M.K. Eghbal [a], J. Givi [b], H. Torabi [c,*], M. Miransari [c,*]

[a] Department of Soil Science, College of Agriculture. Tarbiat Modares University, Tehran, Iran
[b] Department of Soil Science, College of Agriculture. Shahrekord University, Shahrekord, Iran
[c] Department of Soil Science, College of Agricultural Sciences, Shahed University, Tehran, 18151/159, Iran

ARTICLE INFO

Article history:
Received 11 November 2010
Received in revised form 17 October 2011
Accepted 18 October 2011
Available online 25 November 2011

Keywords:
Beach deposits
Gilan
Fragipan
Plinthite
Micromorphology

ABSTRACT

Rice cultivation in the mountainous and sloping areas of Gilan province by leveling and terracing imposes special conditions upon the soils of these areas. Following the retreating Caspian Sea, the beach deposits left in the vicinity of the Elborz Northern foot slopes were covered by fine texture deposits. In this research, macro and micro-morphological characteristics of the soils formed in the Holocene and Pleistocene beach deposits in eastern Gilan, province, were studied. Qualitative and semi-quantitative testing of the soil reduction was carried out by using α,α′-dipyridyl indicator. Free and amorphous sesquioxides were extracted and measured by dithionite-citrate bicarbonate, and oxalate ammonium, respectively. Total Fe, Al, and Mn were measured by digestion. Polished and thin sections were used for micro-morphological description. The most important soil forming process occurring in the Apg and Bg horizons is the formation of depleted, amorphous and cryptocrystalline pedofeatures. The microstructure present in the fragipan and in the horizon characterized by the plinthite properties is mainly pellicular associated with simple packing voids. Coarse/fine (C/F) related distribution shifts from closed chitonic to gefuric. Polished sections show that the opaque minerals of the soils are mostly magnetite (60%) and hematite (40%). Magnetite weathering and its transformation to hematite (martitization process) were also observed. The results of energy dispersive analysis X-ray (EDAX) analyses showed that 40% of the sand grains coatings are iron. Fragipans have been formed in the Late Holocene beach deposits, which are more recent. This occurred when the soils with plinthite characteristics were developed in the Pleistocene beach deposits. Plinthite formation in the Iranian soils was not expected and had not been reported before. Rice cultivation and Anthric saturation may play an important role in plinthite and even fragipan formation in the studied area.

© 2011 Elsevier B.V. All rights reserved.

1. Introduction

Rice is an important crop plant feeding a large number of people in the world. Because of the high rate of precipitation, rice is the main crop and is widely planted in the northern part of Iran nearby the Caspian Sea. However, the way it is planted is different from other crops as it should be grown in a saturated soil. Such conditions can profoundly affect soil properties such as their pedological properties and hence soil efficiency. The pedological properties can also influence rice growth and yield production.

Accordingly, it is important to investigate the effects of different pedological properties on rice yield as well as the effects that rice production can have on the pedological properties of the region. Accordingly, it is of significance to understand soil issues in such regions for a more appropriate use. Some soils of the regions are located on the Sefid Rud river Delta, however, most agricultural lands are located on the deposits (piedmont) of the northern Alborz mountains with a different degree of soil evolution from the Delta soils. Such characteristics are only found in this part of Iran and hence it is important to investigate their properties.

According to Keys to Soil Taxonomy (Soil Survey Staff, 2010), "Plinthite" (Gr. *Plinthos*, brick) is a clay mixture containing quartz and other minerals and low in organic matter and humus. It usually shows redox features with platy, polygonal, or reticulate structures. Plinthite turns irreversibly into a hardpan of iron stone or into aggregates with irregular structures by repeated wetting and drying, especially in the presence of heat from the sun. At about field capacity conditions, plinthite is firm or very firm, however when the soil moisture reduces to below than wilting point it becomes hard. In a moist soil, plinthite can be easily cut with a spade.

Often plinthite has a platy structure with nodular formation (Daniels et al., 1978). The color of platy plinthite bodies is red to yellowish red or dark brown, with a length of about 1 to 4 cm, and is usually oriented horizontally. Although nodular plinthite bodies are similar in their color range, their shape is irregular to spherical. Usually platy plinthite is formed on level landscapes in the presence

* Corresponding authors. Tel.: +98 2151212243.
E-mail addresses: hossien_t@yahoo.com (H. Torabi), Miransari@gmail.com, Miransari@shahed.ac.ir (M. Miransari).

0169-1317/$ – see front matter © 2011 Elsevier B.V. All rights reserved.
doi:10.1016/j.clay.2011.10.013

of a freely fluctuating water table. However, the formation of nodular plinthite apparently takes place on more sloping landscapes where water moves over a restrictive horizon. The presence of plinthite in Iran has not previously been reported in the literature.

Among different diagnostic subsurface horizons, fragipan is the only one whose verification is not possible using solely laboratory analyses. Instead, it can be identified by a series of five field indications (Soil Survey Staff, 2010). According to the last of these indications, after immersion in water, a fragipan clod will slake or fracture.

The strength of particles bonding determines the ability of a fragipan clod to slake, due to its weak physical bonding within the fragipan matrix. According to some researchers amorphous material affects the strength of bonding in a fragipan (Ajmone Marsan and Torrent, 1989; Norton et al., 1984; Steinhardt and Franzmeier, 1979) whereas others have attributed this property to the presence of clay as the main component (De Kimpe et al., 1983). Fragipan is a subsoil horizon with a high density, which is mainly due to the arrangement of silt and sand particles, and is not favorable to plant growth (Bryant, 1989; Norfleet and Karathanasis, 1996; Scalenghe et al., 2004).

According to some researchers, micromorphological properties of fragipan horizons have indicated that argillans form the coatings of

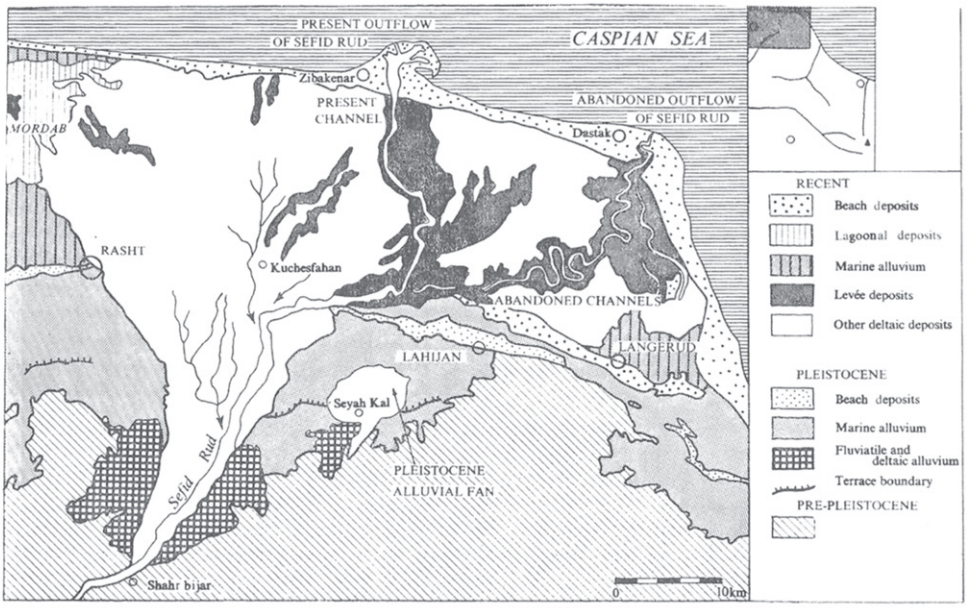

Pleistocene and Recent deposits of the Sefid Rud delta and adjoining parts of the Caspian Plain.

Study location

Map of IRAN

Fig. 1. Guilan province in Northern Iran, South of Caspian Sea, and the geological map of Guilan and the study area (Annells et al., 1975).

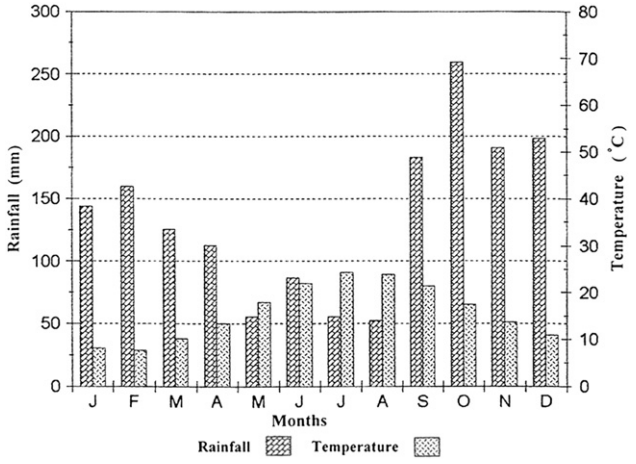

Fig. 2. The distribution of average monthly rainfall and temperature from 1986 to 1996 at Lahijan Meteorological Station, near the study area.

voids as well as the bridges between skeletal grains (Certini et al., 2007; Givi, 1994; Lindbo and Veneman, 1993; Ranney et al., 1975), however, others reported that the formation of bridges between grains is due to amorphous silica (Nettleton et al., 1968; Norton et al., 1984). Givi (1994) reported the occurrence of fragipans in Holocene beach deposits in eastern Gilan Province. The objectives of the present study were to: 1) characterize soils based on their morphological, micromorphological, physical, chemical, and mineralogical properties to identify their formation process, and 2) evaluate the Anthraquic (moisture pattern) effect on the formation of plinthite and fragipan.

2. Materials and methods

2.1. Study area

The study area lies within eastern Gilan province on the northern slopes of the Elborz Range, Iran with a 2 to 5% southern–northern slope (Fig. 1). It is characterized by a humid climate with moderate temperatures. The mean annual temperature of the area is approximately 16 °C, with a difference of 16.5 °C between the coldest and the warmest months. The average annual rainfall in the Langerud and Lahidjan regions is 1605 mm (1990–1999). The mean monthly relative humidity is 75.8%. Fig. 2 shows the mean monthly temperature and rainfall in the area. The geology of the study area has been documented by a generalized geological map prepared by the Iranian National Oil Company (1960) and by Annells et al. (1975). The soils in the region are traced and leveled traditionally for cropping rice.

The lithology of the Elborz Range varies considerably along the east–west direction. However, in the east, it consists mostly of acidic metamorphic and intermediate igneous rocks such as phyllites, quartzites, gneiss, biotite–granite, andesite, and diorite. The plains consist of alluvial material as well as younger Tertiary sediments of the Caspian Sea (Fig. 1). The Pleistocene and early Holocene beach deposits have become observable in Lahidjan and Langerud due to the retreat of the seawater along the northern Elborz Range footslopes (Fig. 1).

2.2. Field methods

Two out of six pedons, which are the representative of soil properties in the region, were selected in Holocene and Pleistocene beach deposits. The morphological characteristics of the soils were described and classified according to Soil Taxonomy (Soil Survey Staff, 2010). Bulk samples were taken from the selected pedons (to the depth of 120 cm) for laboratory analysis, and orientally undisturbed samples were collected for micromorphological study. The presence of plinthite was verified by placing clods in water after being shaken gently for 2 h. The materials which were not slaked by this treatment were considered to be petro-plinthite (Daniels et al., 1978; Wood and Perkins, 1976a). The existence of fragipan, recognized by soil hardness and the destruction of 50% of soil after suspending in water, was verified according to Soil Taxonomy (Soil Survey Staff, 2010).

About 10 km^2 of paddy fields in the northern slopes of Alborz mountains have these kinds of characteristics as a result of the following two reasons. 1) The parental materials and 2) rice cropping, which occur under saturated and hence highly reduced soils. As a result, the reduced iron is transferred to the deeper horizons resulting in the formation of a layer with plinthite properties. The qualitative and semi-quantitative testing of the soil reduction was carried out using α,α′-dipyridyl indicator in freshly broken clods (Childs, 1981).

2.3. Laboratory methods

Laboratory analysis was performed using the fine particles (<2 mm) of the sampled soils. The pH of the samples was determined on a 1:1 mixture of soil/distilled water and soil/$CaCl_2$ 0.01 M by glass electrode (McLean, 1982). Particle size analysis was performed using a centrifuge by the method of Kittrick and Hope (1963). The organic carbon content was determined by the Walkley–Black (wet

Table 1
Selected chemical properties.

Horizon	Depth (cm)	TN (%)	OC (%)	CEC cmol (+) kg^{-1} soil	pH (1,1)		ECe dS/m	CaCo3 (%)	Exch. Acidity cmol (+) kg^{-1}		B.S (%)	Exch. Cations cmol (+) kg^{-1}			
					Water	$CaCl_2$			Al^{3+}	H^+		Ca^{2+}	Mg^{2+}	Na^+	K^+
Profile 1															
Apg	0–10	0.120	3.56	14.76	5.45	5.13	1.54	1.5	0.00	0.095	76.0	0.17	0.17	3.88	6.81
Bg1	10–25	0.056	1.71	13.54	6.67	6.44	1.20	2.0	0.00	0.040	92.0	0.16	0.29	4.22	7.73
Bg2	25–50	0.060	0.53	14.76	6.31	5.87	0.57	2.0	0.02	0.005	82.0	0.17	0.27	4.41	2.27
2Btx1	50–80	0.011	0.21	25.17	6.40	5.86	0.40	2.0	0.00	0.135	71.0	0.32	0.42	6.65	10.40
2Btx2	80–105	0.008	0.26	22.27	6.39	5.99	0.56	2.0	0.00	0.065	74.0	0.32	0.43	5.97	9.64
2Btx3	105–120	–	0.26	18.51	6.93	6.59	0.75	2.0	–	–	81.0	0.23	0.46	5.12	9.15
Profile 2															
Apg	0–15	0.129	3.77	20.20	6.82	6.71	2.20	3.0	0.00	0.025	87.0	0.36	0.19	2.84	13.9
Bg	15–30	0.084	2.40	14.00	5.15	4.92	1.30	0.0	0.04	0.115	61.0	0.16	0.17	2.16	5.74
2BtVl	30–50	0.025	0.10	16.60	6.21	6.04	0.80	0.0	0.00	0.02	69.0	0.30	0.49	3.70	7.01
2Btv2	50–80	0.015	0.00	16.20	6.16	5.81	0.55	1.5	0.00	0.02	71.0	0.26	0.39	4.22	6.73
2Btv3	80–120	–	0.00	10.40	6.60	6.11	0.57	1.5	0.00	0.02	73.0	0.17	0.15	2.81	4.46

B.S. Base saturation.

Table 2
Macromorphological characteristics.

Horizon	Depth (cm)	Dry color	Moist color	Redoximorphic features*	Texture**	Structure***	Semi-quantitative tests for Fe^{2+}	Quantitative tests for Fe^{2+}
Profile 1								
Apg	0–10	2.5 Y 5/3	N4	CD 7.5 YR 5/7 Fe masses around of roots	L	Ivfgr&m	0.2–4	+
Bgl	10–25	2.5 Y 5/3.5	5 Y 5/1	CD 7.5 YR 5/7 Fe masses on ped surface	L	lfabk & m	0.2–4	+
Bg2	25–50	10 YR 5/3.5	10 YR 3/2.5	CD 10 YR 5/6 Fe masses on ped surface	CL-SCL	lfabk		
2Btxl	50–80	7.5 YR 5/6	7.5 YR 5/6	CD 10 YR 5/6 Fe masses on ped surface and CD 10 YR 2.5/1 Mu oxides as spots	SCL	lfabk & sg		
2Btx1	80–105	7.5 YR 5/6	7.5 YR 5/6	MD 10 YR 5/2 Fe masses on ped surface and CD 10 YR 2.5/1 Mn oxides as spots	SCL	lfabk & sg		
2Btx3	105–120	7.5 YR 5/6	7.5 YR 5/6		SCL	lfabk & sg		
Profile 2								
Apg	0–15	2.5 YR 5/3	5 GY 4.5/1.	CD 7.5 YR 5/6 Fe masses around of roots	CL	m	0.2–4	+
Bg	15–30	2.5 YR 5/4	5 GY 4/1	MD 10 YR 5/2 Fe masses on ped surface	L	lf & mabk	0.2–4	+
2Btvl	30–50	7.5 YR 5/6	7.5 YR 4/6	CD 2.5 YR 3/6 and 5 YR 3/3.5 Fe masses mixed with matrix and FD 5 Y 6/1	SCL	2mabk		
2Btvl	50–80	7.5 YR 5/6	5 YR 4/6	CD 5 YR 3/1 Mn oxides as nodules	SCL	2mabk Sg & m		

* Redoximorphic feature abundance M = many (>20%); C = common (2–20%); F = few (2%). Redoximorphic feature contrast; F = faint; D = distinct; P = prominet. ** Texture class; L = loam; CL = clay loam; SCL = sandy clay loam; SL = sandy loam. ***Structure, 2 = moderate; 1 = weak; vf = very fine; f = fine; m = medium; gr = granular; abk = angular blocky; m = massive.

oxidation) method (Nelson and Sommers, 1982). Using the Kjeldahl method total soil N was measured (Nelson and Sommers, 1973). Soil pH and electrical conductivity were also determined (Rhoades, 1982).

Cation exchange capacity and exchangeable cations (K, Na, Mg, and Ca) were measured using the ammonium acetate method (pH = 7.0) (Rhoades, 1982). Ca and Mg of the extracts were determined by an atomic adsorption spectrophotometer. Na and K in the extracts were measured by a flame photometer. The exchangeable acidity (Al^{+3} and H^{+}) was extracted by KF and molar KCl (Robertson et al., 1999; Thomas, 1982).

Free Fe, Al, Mn and Si were extracted using the dithionite-citrate bicarbonate (DCB) method. Oxalate-extractable Fe was obtained by shaking the sample for 4 h in Tamm's acid oxalate solution with a pH of 3.25 (Mehra and Jackson, 1960). Total elemental analyses of the soil samples were carried out using hydrofluoric acid digestion (Lim and Jackson, 1982). The concentration of Al, Fe, Mn and Si was determined by atomic absorption.

2.4. Micromorphological methods

Soil samples were impregnated under vacuum conditions with epoxy resin. Thin sections were prepared and described under a polarizing microscope, using the method of Bullock et al. (1985).

2.5. X-ray analysis

For X-ray diffraction, samples of fine silt (2–5 μm), coarse clay (0.2–2 μm), and fine clay (<0.2 μm) were separated using the methods described by Kittrick and Hope (1963). Coarse and fine clay fractions were analyzed using oriented mounts with the following treatments, Mg-saturation, Mg- and ethylene glycol saturation, K-saturation at 25 °C, K-saturation heated to 300 °C for 2 h, and K-saturation heated to 550 °C for 2 h. The samples were step-scanned from 2° to 36° 2θ. In order to compare the intensity of peaks in different horizons, a portion of the suspension containing 7 mg of fine silt or clay was precipitated on glass slides within the effective beam range of the X-ray diffractometer. Plastic pipes of 2.5 cm in diameter were glued on to surround all glass slides in order to prevent the suspension from flowing over. A given volume of the suspension containing 7 mg of the particles in question was poured on to the glass side and dried at room temperature.

3. Results and discussion

3.1. Macromorphology and physico-chemical properties

Profile 1 is located in the eastern part of the Holocene beach deposits to the South of the Langerud marshland (Fig. 1). These older

Table 3
Particle size distribution.

Horizon	Depth (cm)	Sand (%) mm					Silt (%) mm			Clay (%) mm		Sand (%)	Silt (%)	Clay (%)
		1–2	|0.5–1|	|0.25–0.5|	|0.1–0.25|	|0.02–0.1|	|0.005–0.02|	|0.002–0.005|	|0.005–0.002|	|0.002–0.0002|	<0.0002			
Profile 1														
Apg	0–10	0.10	0.30	3.50	30.94	7.56	13.50	16.25	3.85	9.75	14.25	42.40	33.60	24.00
Bg1	10–25	0.51	0.32	3.00	31.92	5.25	15.75	14.45	4.80	10.25	13.75	41.00	35.00	24.00
Bg2	26–50	0.09	0.05	3.00	38.82	3.84	9.85	11.25	5.10	11.78	16.22	45.80	26.20	28.00
2Btxl	50–80	0.00	0.05	3.65	43.10	5.20	4.89	5.65	3.26	16.65	17.35	52.20	13.80	34.00
2 Btx2	80–105	0.00	0.01	4.00	48.25	6.14	4.02	6.00	3.58	11.00	13.00	58.40	13.60	28.00
2Btx3	105–120	0.00	0.01	4.12	60.25	6.22	3.85	4.10	1.45	7.85	12.15	70.60	9.40	20.00
Profile 2														
Apg	0–15	0.09	0.25	2.42	21.94	5.14	18.87	20.81	5.49	7.35	17.70	29.84	45.17	25.05
Bg	15–30	0.31	0.31	2.29	22.86	5.83	21.21	18.89	3.70	6.71	18.42	31.60	43.27	25.13
2Btvl	30–50	0.01	0.03	2.25	37.72	.82	8.66	12.11	4.44	14.47	15.83	44.49	25.21	30.30
2Btv2	50–80	0.00	0.03	2.76	50.15	5.69	8.07	7.70	2.92	11.42	11.26	58.63	18.69	22.68
2Btv3	80–120	0.00	0.03	4.12	65.42	5.56	5.95	4.25	1.75	6.33	6.59	75.13	11.95	12.92

Table 4
Different forms of Fe, Al, Mn and Si (mg/kg).

Horizon	Depth	Fe_t	Al_t	Mn_t	Fe_d	Al_d	Mn_d	Si_d	Fe_o	Al_o	Mn_o	Si_o	Fe_d–Fe_o
Profile 1													
Apg	0–10	29.0	59.0	0.27	9.31	0.48	0.17	0.75	4.86	0.48	0.07	0.65	4.45
Bg1	10–25	–	–	–	20.81	0.99	0.33	0.59	4.86	0.68	0.14	0.42	15.95
Bg2	25–50	46.0	59.0	1.65	30.06	2.39	0.95	0.66	4.20	2.10	0.56	0.60	25.86
2Btx1	50–80	–	–	–	27.53	2.04	2.18	1.01	6.16	1.25	1.70	0.75	21.37
2Btx2	80–105	48.0	61.0	2.50	26.96	1.95	1.32	1.11	5.30	1.25	0.85	0.74	21.39
2Btx3	105–120	37.0	57.0	0.85	15.81	0.96	0.27	0.87	5.20	0.81	0.10	0.51	10.61
Profile 2													
Apg	0–15	24.0	57.0	0.37	9.85	1.02	0.16	1.04	5.44	1.00	0.16	1.09	4.41
Bg	15–30	26.0	66.0	0.30	10.27	0.87	0.11	0.74	6.28	0.95	0.12	0.75	3.99
2Btv1	30–50	63.0	80.0	1.28	42.75	2.77	0.83	0.51	6.84	1.90	0.80	0.40	35.91
2Btv2	50–80	57.0	78.0	1.41	24.85	1.46	0.76	0.63	7.20	1.05	0.71	0.45	17.55
2Btv3	80–120	43.0	92.0	0.61	19.67	0.96	0.30	0.58	6.70	0.90	0.25	0.44	12.57

T = Total.
D = Citrate- Bicarbonate Dithionite o = Ammonium oxalate.

deposits are covered with a layer of alluvial deposits with varying depths at different points. Tables 1–4 show the morphological and physico-chemical properties. The surface of this soil is covered with water for most of the year. The surface horizon (Apg) in the soil is completely reduced and has a gray color. Except for this layer, no other layer is found down to a depth of 120 cm to be completely in a reducing condition (Table 2). The amount of sand increases from 42.4% in the surface layer to 52.2% in the $2Btx_1$ horizon. The age of

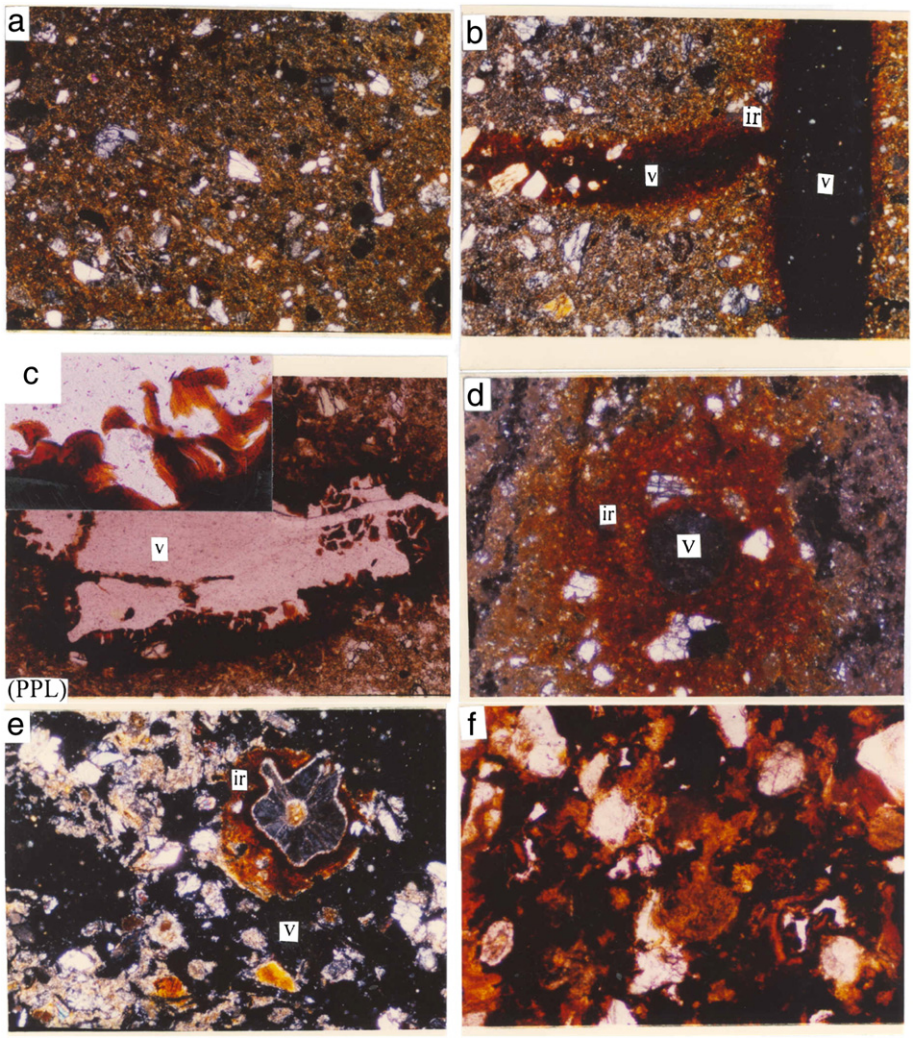

Fig. 3. Thin section of micrographs; (a) massive microstructure in Apg horizon, frame length 2.5 mm, (b), (c) hypo-coating of iron oxides around office root and roodet and channel voids, frame length 2.5 and 1 mm respectively, (d) crystalline iron oxy-hydroxide around chamber void, frame length 2.5 mm, (e) plaque iron or coating of iron oxides around fresh rice root, frame length 2.5 mm, (f) Fe/Mn oxides in nodular plinthite, frame length 1 mm. (All images are cross polarized) v = void; ir = coating or hypo-coating of iron oxides.

deposits is different in the two horizons and there is an abrupt difference in the amounts of soil particles including sand, silt and clay in the two layers.

The amount of clay also increases with depth, reaching its maximum in the $2Btx_1$ horizon (Table 3). Clay coatings are not easily detectable in the field, but micromorphological descriptions reveal clay coatings to a large extent. In the surface horizon with a gray matrix color, precipitated iron oxides are observed around root channels and in the Bg_1 and Bg_2 horizons, mainly on the surface of peds or between planar voids. In the $2Btx_1$ and $2Btx_2$ horizons grayish strata with the dark gray color (5Y4/1) are seen around the channels and between the planar voids. No color changes were observed in these strata after testing with α,α′-dipyridyl indicator. It may be inferred that these grayish strata might have been bleached areas, formed as a result of the depletion of clay and iron oxides.

Chemical analyses showed considerable increases in total and extractable Fe, Al, Mn, and Si in Bg_2, $2Btx_1$, and $2Btx_2$ horizons as compared with the surface horizons (Table 4). Clods of this soil possess characteristics similar to fragipans in that they harden upon air-drying and become brittle after being wetted again. Referring to the increasing amounts of free iron oxide (Fed), Ald, Mnd, and Sid in $2Btx_1$ and $2Btx_2$, it seems that, in addition to silica, other factors, such as sesquioxides in the fragipan horizons, must be considered as cementing factors.

Profile 2 lies on the same Pleistocene beach deposits located between Langerud and Lahidjan townships (Siahkal-deh) (Fig. 1). In this soil, under the plow layer (Apg), there is an extremely reduced grayish compact layer (Bg) formed as a result of puddling operations. Such a low permeable layer was not observed in profile 1. These deeper horizons are similar to the profile 1 with regard to sand content and the aerobic (oxidation) conditions. Since this soil, and the older beach deposits, lies alongside the edges of the mountain (at a distance of 100 to 200 m from the knickpoint of the Elborz Mountains), the water table in these soils has greater fluctuation as compared to a groundwater in plain soils. Therefore, the completely reduced layer has not been formed in lower depths in these soils. The water table in these areas is generally deeper than 1.5 m throughout the year.

The mechanism of saturation and reduction in this soil is of the 1B kind in the Fanning Model (Fanning and Fanning, 1989), in which Fe^{+2} is produced in the upper layers with finer texture and higher degradable organic material and then diffuses into subsurface layers (from Apg to Bg and from Bg to the deeper layers), which have more aerobic conditions (particularly the lower sand horizons). Due to abundant oxygen in these layers, Fe^{+2} is oxidized and then precipitates. This process in the reducing layer decreases the Eh value and gradually exhausts the iron oxides present. Under such conditions, the formation of plinthite in the layers with coarse textures will become possible (Fanning and Fanning, 1989).

The surface horizon Apg and the Bg horizon have been completely reducing conditions (McDaniel et al., 2008). Iron oxides are accumulated around rice roots in the surface horizon but decayed roots are seen on the ped surfaces (in planar voids) and in the channel voids in the Bg horizon. Reduced manganese and iron are abundantly diffused, particularly in the Bg horizon, into the subsurface layers where, due to the existence of an adequate supply of oxygen and a fine soil texture, they are oxidized and then precipitate. The continuation of the process causes the hardening of the underlying horizons so that, despite the wetness of the soil, sampling from the underlying horizons is difficult. Clods from the third (Bg2) and fourth (2Btxl) horizons were not brittle even when wet.

The plinthite formed in this soil is of the nodular type. Daniels et al. (1978) reported the possibility of the formation of such plinthites on sloping landscapes with more horizontal water flows. The nodules separated from the body of the horizons, generally larger than 30 mm in diameter, were placed in water for 2 h after being air-dried. The nodules did not break even after wetting.

As in profile 1, the clay coatings were observed in micromorphological studies of all the three $2Btv_1$, $2Btv_2$ and $2Btv_3$ horizons. The clay contents in $2Btv_2$ and $2Btv_3$ are 22% and 13%, respectively, which are 8% and 17% less than the clay contents in Btv_1. These two

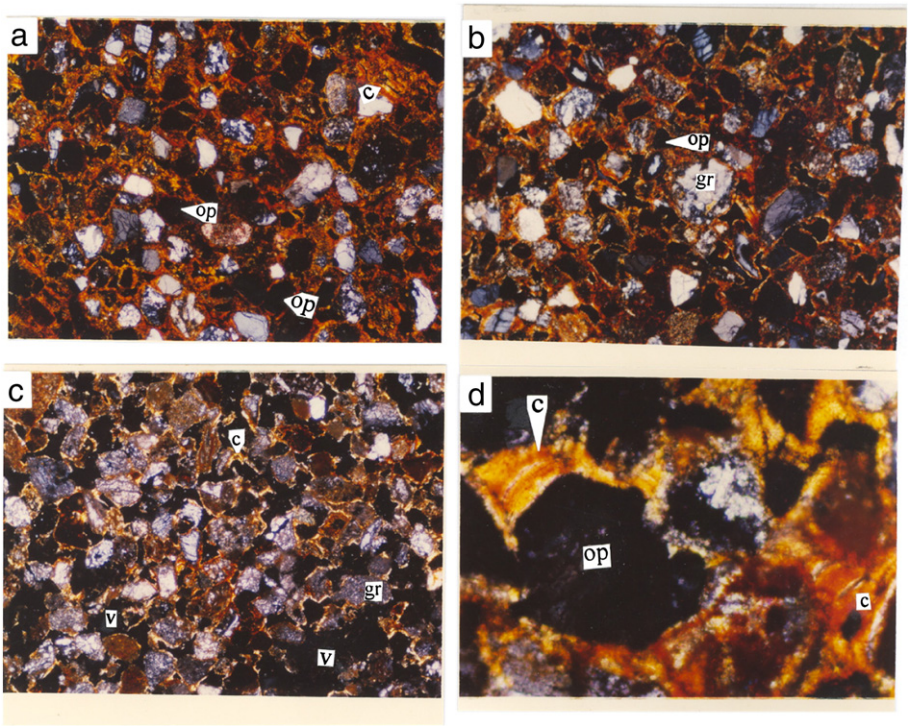

Fig. 4. Photomicrographs of clay coatings in profile no. 2. (a) chitonic and closed porphyric distribution in Btv1 horizon, frame length 2.5 mm, (b) chitonic distribution in Btv2 horizon, frame length 2.5 mm, (c) chitonic and gefuric and some enaulic distribution in Btv3 horizon, frame length 2.5 mm, (d) clay coatings around opaque mineral, frame length 0.5 mm. (All images are cross polarized). v = void; gr = sand grain; c = clay coating; op = opaque mineral.

horizons, however, are called argillic because if horizons like $2Btv_3$ are considered sandy horizons and if we further suppose the total clay content in them as transported clay, then they have a transported clay content of at least 10% when compared to their original states (Table 3). This horizon can be regarded as argillic despite its clay content being lower by a few percent in comparison to its overlying horizon. Such details are verified by the following observations: 1) a clay film connecting sand particles like a bridge, and 2) more than 1% clays traced in thin microscopic sections (Fig. 4). Because of the less effective movement of moisture front to the deeper layers, a higher concentration of clay is found in the upper layers. However, although the deeper layers have smaller amounts of clay (Btv1), the clay films are observable among them (Fig. 4). Gray strata are observed to about 5% along channels internal surfaces and on the surface of some peds in $2Btv_1$ to $2Btv_3$ horizons similar to profile 1. These strata do not respond positively to Fe^{+2} tests.

The total amounts of Fe, Al, and Mn increase with increasing depths, particularly in $2Btv_1$ to $2Btv_3$ horizons (Table 4). The free iron oxide (Fed) in the $2Btv_1$ horizon is almost four times its concentration in Apg and Bg horizons. No increasing trend is observed in the quantity of silica in the plinthite horizons. Therefore, it can be concluded that iron and perhaps aluminum play more important roles in the hardening process in these horizons. At the same time, great quantities of Mn have been found in the nodules, which respond vigorously to 30% H_2O_2 at room temperature. The same trend is observed in profile 1, the only difference being that the quantity of Fe_d in the fragipan is not even twice its quantity in Apg, Bg_1 or Bg_2 horizons. Wood and Perkins (1976b) studied the characteristics of some plinthites in coastal plain soils. According to these authors, the mineralogical composition of plinthites included quartz, hematite, goethite and some poor crystalline kaolinite. They found the quantity of iron oxide to be two to three times its quantity in the overlying layers.

3.2. Micromorphology

Due to puddling operations, the microstructure of surface horizons, particularly at the depths of 5 to 20 cm, is massive (Fig. 3a) and the corresponding voids are partly of the vesicle type and partly in the form of channels left by decayed roots. The greatest concentration of rice roots was observed at the depths of 0 to 50 cm. The most significant pedological phenomena in this horizon consist of depletion and amorphous material formation. The depletion phenomenon accounts for 20 to 25% of the section with an average thickness of 100 to 800 μm with diffuse boundaries (several soil samples were collected from horizons and cut on different sides as shown in the figures). Around 10 to 15% of the horizon is occupied by accumulated amorphous materials and cryptocrystalline materials as coatings and hypocoatings with varying degrees of coverage. Accumulated iron oxides in the form of hypo-coating around the rice rootlets are shown in Fig. 3b, d and e. The hypo-coating at shorter distances from the voids is strongly impregnated whereas at greater distances there is no clear boundary so that the soil matrix is weakly impregnated (Fig. 3c).

The iron oxide crystals, probably goethite or lepidocrocite, on the walls of channel and chamber voids, have grown perpendicular to the void walls and have an extinction angle. Mineralogical studies of the iron oxide coating around rice roots and on the channel void walls confirmed the existence of the above minerals (Torabi et al., 2000). The micromorphological characteristics of the Bg horizon are similar to those of the Apg horizon, the major differences being a completely gray matrix in the former, little plant remains, and more accumulated iron oxides on channel and planar void walls and more iron oxides as soft nodules (Fig. 3c).

Due to presence of considerable sand particles in the $2Btv_1$ to $2Btv_3$ and $2Btx_1$ to $2Btx_3$ horizons, the clay coating is perfectly visible under the microscope. The microstructure in these horizons is basically of the Pellicular type while the voids are simply packed. The coarse/fine (C/F) related distributions in the $2Btv_1$ and $2Btx_1$ horizons are typically Chitonic, shifting to Gefuric towards the lower parts of the $2Btv_2$ and $2Btx_2$, and particularly in the $2Btv_3$ and $2Btx_3$, horizons.

The illuviated clay in argillic horizons is generally in the following forms,

1. As coating surrounding all or part of the mineral particles;
2. As bridges between the mineral particles; and
3. As coating on walls of some of the voids, particularly the channel voids.

The quantity and thickness of the clay coatings greatly reduces from $2Btv_1$ and $2Btx_1$ horizons towards $2Btv_3$ and $2Btx_3$ horizons (Fig. 4a, b and c).

In sandy soils, the pore space is mainly composed of more or less continuous simple packed voids. In the argillic horizon of such soils, the grains are coated and more or less bridged by illuvial clay. These

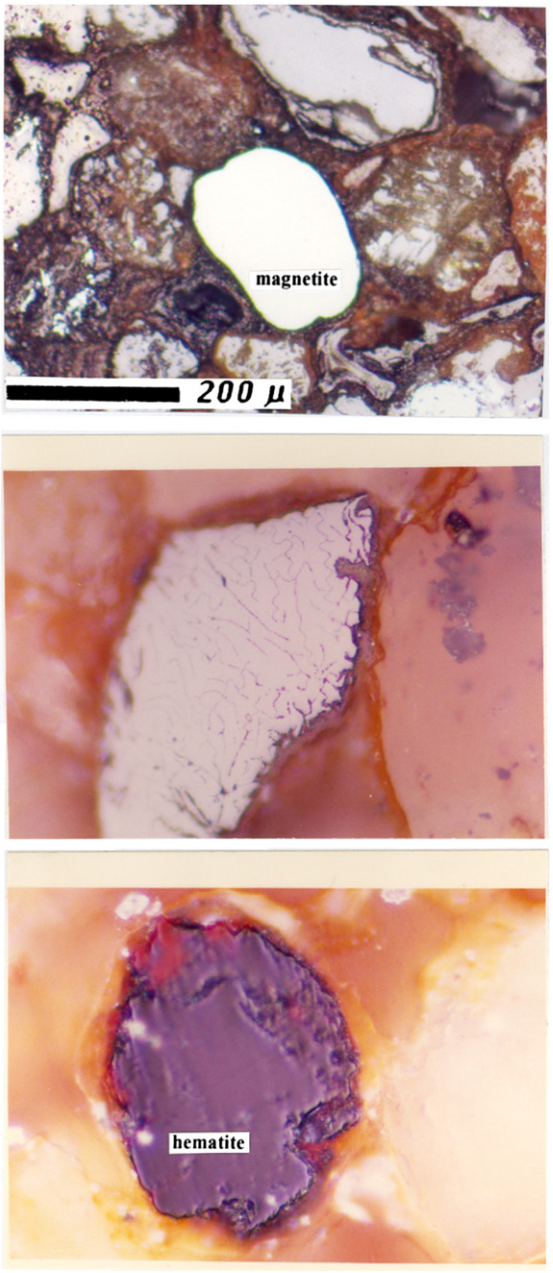

Fig. 5. Polished section of micrographs; (a) magnetite, plane polarized; (b) transformation of magnetite to hematite (Martitization) as black strings, plane polarized, frame length 1 mm; (c), hematite, cross polarized, frame length 0.25 mm.

coatings usually show a strong birefringence, but in some soils, the coatings may be mixtures of different particles, resulting in lower birefringence. The case in which strongly oriented clay particle coat and bridge mineral grains in coarse textured material is an example of a clearly identifiable argillic horizon (Bullock and Thompson, 1985).

The presence of well-oriented clays around grains is usually recognizable in thin sections (Fig. 4a, b and d). The reddish clay coating around the grains is rich in iron. The EDAX analysis of these coatings revealed iron contents of up to 40% while the treatment of the thin sections by DCB eliminated the iron oxides around grains and caused bleaching of the clay coatings. After the use of hydrogen peroxide (H_2O_2) the dark spots in these sections were identified using microscopy. If there is a speedy reaction the spots are manganese oxide (MnO_2) otherwise they are organic matter.

In the $2Btv_1$ and $2Btv_2$ horizons, the clay coatings around the grains are superimposed by amorphous black colored Mn oxide (Fig. 3f). The treatment of this black coating with 30% H_2O_2 at laboratory temperature caused its strong reaction and removal, leading to uncovered clay coatings. However, it seems that strong saturation causes the formation of nodules, as large as 30 mm or larger, which are detected as dark colored spots in profile description, and can be separated from the soil matrix of the profile.

Mineralogical analyses of the polished samples revealed that the major opaque minerals present in these soils include around 60% magnetite (Fe_3O_4) and 40% hematite (Fe_2O_3). The analyses was performed using undisturbed clods, which were saturated with resin and polished with corundum powder (Al_2O_3). The samples were then observed with polarizing microscopy and according to their reflection the opaque minerals were indentified. The minerals had the same size as the sand grains in Pleistocene sediments. Magnetite and hematite in polished sections appear in plane polarized light as brilliant white without pleochroism (Fig. 5a). However, in crossed polarized light, magnetite appears without extinction angles and acts as isotropic

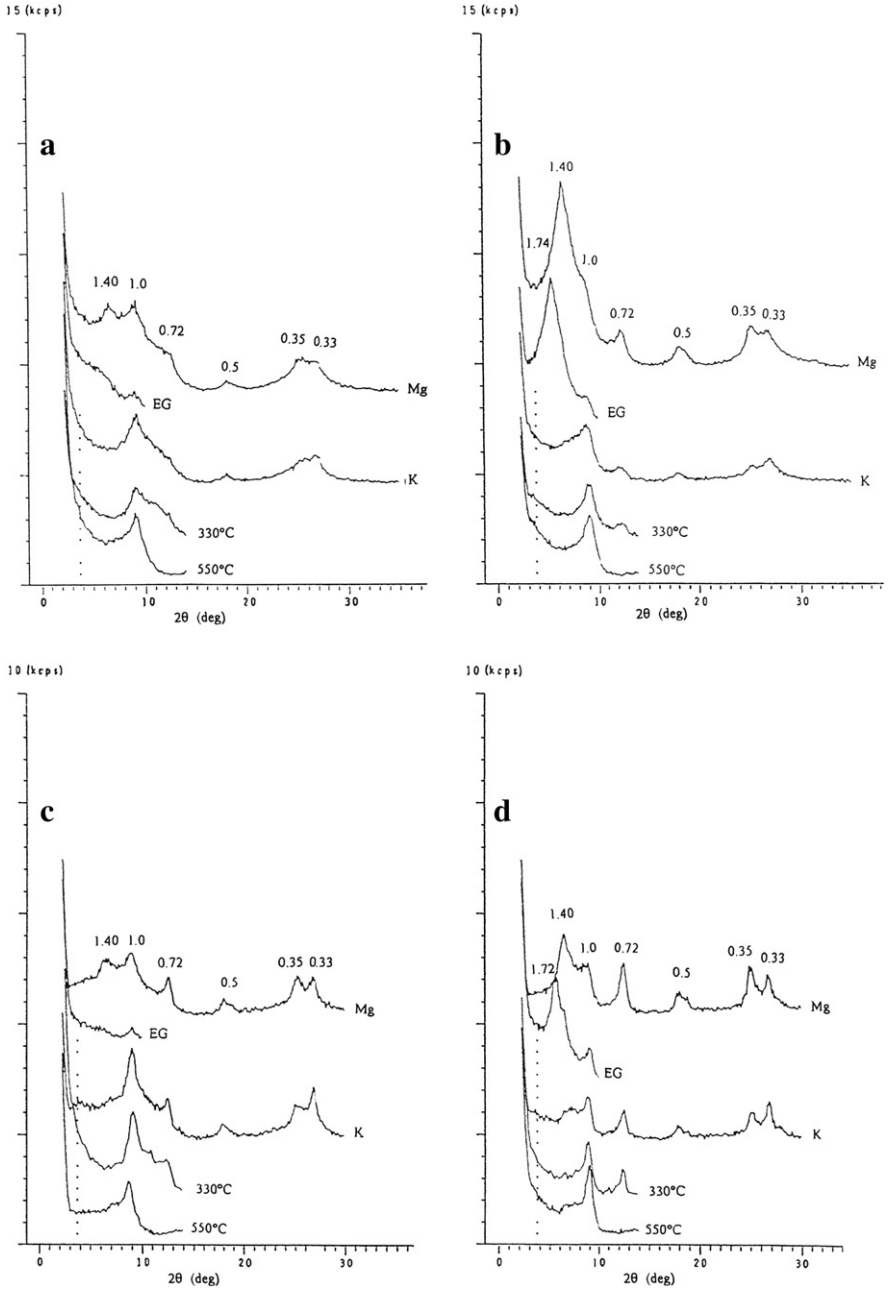

Fig. 6. X-ray diffraction patterns of clay of the profile no. 2; (a) fine clay of Apg horizon, (b) coarse clay of Apg horizon, (c) fine clay of Btv1 horizon, (d) coarse clay of Btv1 horizon.

minerals while hematite has an extinction angle (Fig. 5c). The martitization phenomenon is recognizable in some magnetite grains. In such cases, hematite is found as strings or narrow strips in the magnetite (Fig. 5b) (Swanson-Hysell et al., 2011). The continuation of this trend causes the weathering of the magnetite into hematite and hence, to other iron hydroxide minerals.

3.3. Mineralogical analysis

The mineralogical study of the clay fraction of these soils revealed considerable differences between the Apg and Bg horizons, on one hand, and fragipan and plinthite on the other hand. In the fine clay fraction of the Apg and Bg horizons, the smectite mineral peak is generally sharp and strong, which indicates the presence of smectites with good crystallinity (Fig. 6a and c). The same situation prevails in the coarse clay, with the difference that the intensity of the smectite peak reduces and that evidence can be found indicating the presence of minerals with inter-layer hydroxides or an irregular mixture of chlorite–smectite, chlorite–vermiculite, and chloride–mica (Fig. 6b and d). In the fine and coarse clay fractions of the plinthite and fragipan horizons, however, the 1.4 nm peak was not a distinct after treating with ethylene glycol vapor, a condition indicating smectites with low crystallinity (Fig. 6c).

4. Conclusion

In our study area, formation of fragipan and plinthite is strongly affected by anthraquic conditions. Leveling and terracing for rice cultivation accelerate these processes. Parent material and burial of coarse-textured beach deposits by heavy-textured alluvial deposits (lithological discontinuity) could also be affected by these processes. Mn^{+2} and Fe^{+2}, formed in the fine-textured upper layers (Apg and Bg horizons) due to saturation and reduction of those layers, were diffused into coarse-textured underlying layers (old beach deposits), which are more aerobic. Due to the presence of enough oxygen in these layers, Mn^{+2} and Fe^{+2} are oxidized and then precipitate. The fragipan horizon has been mostly formed in the late Holocene beach deposits, which are more recent. This is in the case that the soils with plinthite characteristics have been developed in some of the Pliestocene beach deposits. The results have shown that the fragipan, which is transforming to plinthite, has a nodular form with an irregular to spherical shape. We believe that amorphous material (sesquioxides) and some clay were the main components related to the bonding of fragipan. In older geological formations, due to iron leaching, the probability of plinthite formation in soil was more likely than in the younger formations.

Acknowledgment

The authors would like to thank Jihad-Agricultural Research and Education for their support of this project.

References

Ajmone Marsan, F.A., Torrent, J., 1989. Fragipan bonding by silica and iron oxides in a soil from northwest Italy. Soil Science Society of America Journal 53, 1140–1145.
Annells, R.N., Arthurton, R.S., Bazly R.A., Davies, R.G., 1975. Explanatory text of the Qazvin and Rasht quadrangles map 1,250,000. Geological Survey of Iran, Geological Quadrangles Nos E3, E4, 94p.
Bryant, R.B., 1989. Physical processes of fragipan formation. In: Smeck, N.E., Ciolkosz, E.J. (Eds.), Fragipans: their occurrence, classification, and genesis. : SSSA Spec. Pub., 24. SSSA, Madison, WI, pp. 141–150.
Bullock, K.P., Thompson, M.L., 1985. Micromorphology of Alfisols. In: Douglas, L.A., Thompson, M.L. (Eds.), Soil Micromorphology, Soil Classification: SSSA Special Publication Number 15, pp. 17–47. Madison, WI.
Bullock, P., Fedoroff, A., Jongerius, A., Stoops, G., Tursina, T., 1985. Handbook for Thin Section Description. Waine Research Publications, Albrighton, U.K.
Certini, G., Ugolini, F.C., Taina, I., Bolla, G., Corti, G., Tescari, F., 2007. Clues to the genesis of a discontinuously distributed fragipan in the northern Apennines, Italy. Catena 69, 161–169.
Childs, C.W., 1981. Field test for ferrous iron and ferric organic complexes (on exchange sites or in water-soluble forms) in soils. Australian Journal of Soil Research 19, 175–180.
Daniels, R.B., Perkins, H.F., Hajek, B.F., Gambel, E.E., 1978. Morphology of discontinuous phase plinthite and criteria for its field identification in the Southern United States. Soil Science Society of America Journal 42, 944–949.
De Kimpe, C.R., Laverdiere, M.R., Dejoue, J., 1983. Distribution of silica, sesquioxides, and clay in Quebec podzolic soils and their effects on subsoil cementation. Soil Science Society of America Journal 47, 838–840.
Fanning, D.S., Fanning, M.C.B., 1989. Soil, Morphology, Genesis, and Classification. John Wiley & Sons, New York.
Givi, J., 1994. Genesis and characteristics of representative alluvial soils from different climatic zone in Iran. Ph.D. thesis, State Univ. Ghent, Belgium, 407p.
Iranian National Oil Company. 1960. Generalized geological map of Iran.1,1,000,000 and 1,250,000, Sheets Nos. 1 and 2.
Kittrick, J.A., Hope, E.W., 1963. A procedure for the particle size separation of soils for X-ray diffraction analysis. Soil Science 96, 319–325.
Lim, C.H., Jackson, M.L., 1982. Dissolution for total elemental analysis, In: Page, A.L., Miller, R.H., Keeney, D.R. (Eds.), Methods of soil analysis. Part 2, 2nd ed. : Agron. Monogr., 9. ASA and SSSA, Madison,WI, pp. 1–110.
Lindbo, D.L., Veneman, P.L.M., 1993. Morphological and physical properties of selected fragipan soils in Massachusetts. Soil Science Society of America Journal 57, 429–436.
McDaniel, P.A., Regan, M.P., Brooks, E., Boll, J., Barndt, S., Falen, A., Young, S.K., Hammel, J.E., 2008. Linking fragipans, perched water tables, and catchment-scale hydrological processes. Catena 73, 166–173.
McLean, E.O., 1982. Soil pH and lime requirement, In: Page, A.L., Miller, R.H., Keeney, D.R. (Eds.), Methods of soil analysis. Part 2, 2nd ed. : Agron. Monogr., 9. ASA and SSSA, Madison, WI, pp. 199–224.
Mehra, O.P., Jackson, M.L., 1960. Iron oxide removal from soils and clays by a dithionite–citrate system buffered with sodium bicarbonate. Clays and Clay Minerals 7, 317–327.
Nelson, D.W., Sommers, L.E., 1973. Determination of total nitrogen in plant material. Agronomic Journal 65, 109–112.
Nelson, D.W., Sommers, L.E., 1982. Total carbon, organic carbon, and organic matter, In: Page, A.L., Miller, R.H., Keeney, D.R. (Eds.), Methods of soil analysis. Part 2, 2nd ed. : Agron. Monogr., 9. ASA and SSSA, Madison, WI, pp. 539–577.
Nettleton, W.D., McCracken, R.J., Daniels, R.B., 1968. Two North Carolina coastal plain catena, II. Micromorphology, composition and fragipan genesis. Proceedings. Soil Science Society of America 32, 582–587.
Norfleet, M.L., Karathanasis, A.D., 1996. Some physical and chemical factors contributing to fragipan strength in Kentucky soils. Geoderma 71, 289–301.
Norton, L.D., Hall, G.F., Smeck, N.E., Bigham, J.M., 1984. Fragipan bonding in a late-Wisconsin loess-derived soil in east central Ohio. Soil Science Society of America Journal 48, 1360–1366.
Ranney, R.W., Ciolkosz, E.J., Cunningham, R.L., Petersen, G.W., Matelski, R.P., 1975. Fragipans in Pennsylvania soils, properties of bleached prism face materials. Proceedings. Soil Science Society of America 39, 695–698.
Rhoades, J.D., 1982. Soluble salts, In: Page, A.L., Miller, R.H., Keeney, D.R. (Eds.), Methods of soil analysis. Part 2, 2nd ed. : Agron. Monogr., 9. ASA and SSSA, Madison, WI, pp. 167–179.
Robertson, G.P., Sollins, P., Ellis, B.G., Lajtha, K., 1999. Exchangeable ions, pH, and cation exchange capacity. In: Robertson, G.P., Bledsoe, C., Coleman, D., Sollins, P. (Eds.), Standard Soil Methods for Long-Term Ecological Research. Oxford University Press, New York, pp. 106–114.
Scalenghe, R., Certini, G., Corti, G., Zanini, E., Ugolini, F., 2004. Segregated ice and liquefaction effects on compaction of fragipans. Soil Science Society of America Journal 68, 204–214.
Soil Survey Staff, 2010. Keys to soil taxonomy, Eleven edition. United States Department of Agriculture and Natural Resources Conservation Service. U.S. Government Printing Office, Washington, DC.
Steinhardt, G.C., Franzmeier, D.P., 1979. Chemical and mineralogical properties of the fragipans of the Cincinnatic catena. Soil Science Society of America Journal 43, 1008–1013.
Swanson-Hysell, N.L., Feinberg, J.M., Berquó, T., Maloof, A., 2011. Self-reversed magnetization held by martite in basalt flows from the 1.1-billion-year-old Keweenawan rift, Canada. Earth and Planetary Science Letters 305, 171–184.
Thomas, G.W., 1982. Exchangeable cations. In: Page, A.L., Miller, R.H., Keeney, D.R. (Eds.), Methods of soil analysis. : Agron. Monogr., 9. ASA, Madison, WI, pp. 159–165.
Torabi, H., Eghbal, M.K., Givi, J., 2000. Characteristics of iron coatings formed on rice roots in paddy soil of eastern Guilan, Iran (in Persian). Iranian Journal of Soil Water Science 14, 121–129.
Wood, B.W., Perkins, H.F., 1976a. A field method for verifying plinthine in southern coastal plain soils. Soil Science 122, 240–241.
Wood, B.W., Perkins, H.F., 1976b. Plinthite characterization in selected southern coastal plain soils. Soil Science Society of America Journal 40, 143–146.